12.7 OCEAN FRONTS AROUND ALASKA FROM SATELLITE SST DATA

Igor M. Belkin*, Peter Cornillon and David Ullman
University of Rhode Island, Narragansett, Rhode Island

ABSTRACT

Long-term time series of satellite observations are used to survey ocean surface thermal fronts in the Gulf of Alaska, Bering, Chukchi and Beaufort Seas as well as in the upstream region of the Alaskan Current and farther south along the North American shelf to include British Columbia waters and the Columbia River Plume area, thus covering 45°N-75°N, 160°E-120°W. The Cayula-Cornillon algorithms for front detection and cloud screening were applied to the Pathfinder twice-daily 9-km resolution SST images from 1985-1996. A number of new frontal features have been identified in the Alaskan Seas; some previously known fronts have been systematically studied for the first time. Frontal frequency maps are provided for each of four Alaskan Seas. In the Gulf of Alaska and Bering Sea the SST fronts are best defined in spring (May) and fall (November), while being masked by surface heating in summer. In the Chukchi and Beaufort Seas the SST fronts are best seen in summer (August-September), when both seas are typically ice-free. Seasonal evolution of SST fronts is noted off the Oregon-Washington coasts and Vancouver Island, in Hecate Strait and Dixon Entrance.

INTRODUCTION

Ocean fronts are relatively narrow zones of enhanced horizontal gradients of physical, chemical, and biological properties that separate broader areas of different vertical structure (stratification). The fronts are crucial in various processes that evolve in the ocean and at the ocean interfaces with the atmosphere, sea ice and ocean bottom (Belkin, 2003a, b). Until the 1970s, frontal studies were based on ship data (Fedorov, 1986). The main problem in using ship data for climatological purposes is extremely non-uniform, patchy, and mostly sparse coverage provided by ship data. On the contrary, satellite data, at least, in principle, are spaced regularly and allow a fairly dense global coverage to be attained. The satellite data sets extend back to the early 1980s, thus encompassing nearly two decades and allowing a long-term variability of fronts to be studied. Satellite-retrieved sea surface temperature (SST) data have been widely used for regional frontal studies since the 1970s (e.g. a global survey of Legeckis, 1978). Earlier studies (see extensive bibliographies in Belkin et al., 2003a,b,c) have been focused mainly on fronts associated with western boundary currents such as the Gulf Stream, Kuroshio, Brazil-Malvinas Confluence, Agulhas Current, and East Australian Current; fronts associated with eastern boundary currents and coastal upwellings have been studied in such areas as the California Current, Peru-Chile Current, Canary Current and Northwest African upwelling, Benguela Current, and Leeuwin Current; in the open ocean, the North Atlantic Subtropical Front and the North Pacific Subtropical Front received most attention, while high-latitude fronts masked by persistent cloudiness have nonetheless been studied in the Nordic Seas and the Southern Ocean.

Satellite observations of surface fronts in high-latitude seas are hampered by seasonal ice cover and persistent cloudiness. Nonetheless, several studies have demonstrated the great potential of remote sensing, including infrared imagery, in observing surface manifestations of oceanic phenomena (fronts, eddies, upwelling etc.) such as the Warm Coastal Current in the Chukchi Sea (Ahlnäs and Garrison, 1984), coastal upwelling off St. Lawrence and St. Matthew islands in the Bering Sea (Saitoh et al., 1998), the St. Lawrence Island Polynya (SLIP; Lynch et al., 1997), and spring blooming in the Bering Sea (Maynard and Clark, 1987; Walsh et al., 1997).

The above studies, being very important in elucidating physics and geography of individual fronts, didn't amount however to a regional synthesis, which requires a unifying approach to be consistently applied to a long-term data set of thoroughly calibrated measurements. The present work summarizes the most important results of such a project undertaken at the University of Rhode Island (URI), where advanced algorithms for front detection and cloud screening have been developed earlier, described in the next section.

The present work is essentially an *exploratory* study. The main goal is to describe *all* the robust (persistent) frontal features noticeable in the data, regardless of the spatial scale of the features, and

**Corresponding author address:* Igor M. Belkin, Univ. Rhode Island, Grad. School of Oceanography, 215 S. Ferry Road, Narragansett, RI 02882, email: ibelkin@gso.uri.edu

compare them with previously available observations. As such, the work presents a brief provisional compendium of thermal fronts observed in the Alaskan seas.

DATA AND METHOD

Because the fronts are originally defined as high-gradient zones, most objective computer-based approaches to front identification are based on gradient computations (e.g. Kazmin and Rienecker, 1996; Yuan and Talley, 1996). The approach used in this study is based on ***histogram analysis***. Since a front is a boundary between two relatively uniform water masses, histograms of any oceanographic characteristic (e.g. SST) in the vicinity of the front should have two well-defined modes that correspond to the water masses divided by the front, while the latter corresponds to the frequency minimum between the modes. This basic idea has been implemented by Cayula and Cornillon (1992, 1995, 1996) and Ullman and Cornillon (1999, 2000, 2001); the reader is referred to these works for pertinent details. The fronts used for this study were derived from the NOAA/NASA Pathfinder SST fields (Vazquez et al., 1998) for the period 1985-1996, covering almost entire World Ocean, from 75°N to 75°S. These fields were obtained from the AVHRR Global Area Coverage data stream (two 9.28-km resolution fields per day) and are available from the Jet Propulsion Laboratory. SST fronts were obtained from the cloud-masked SST fields with the multi-image edge detection algorithm (Cayula and Cornillon, 1996; Ullman and Cornillon, 1999, 2000, 2001). The cloud masking and front detection algorithms were applied to each of the 8364 SST images in the 12-year sequence. The frontal data were aggregated over months (e.g. 12 Januaries taken together), and seasons (e.g., the winter climatology is obtained from all Januaries, Februaries, and Marchs taken together). The front detection and tracking is conducted at three levels: window, image and a sequence of overlapping images. The optimum window size is important. Based on a series of numerical experiments with various window sizes, Cayula and Cornillon (1992) have arrived at the optimum window size of 32 by 32 pixels. The front detection algorithm uses all pixel-based SST values within each window to compute a SST histogram for the given window. For each window that contains a front (a relatively narrow zone of enhanced SST gradient), the corresponding SST histogram would have a frequency minimum identified with the front. Three basic types of maps are used in the analysis: *long-term frontal frequency maps*, *quasi-synoptic frontal composite maps*, and *long-term frontal gradient maps*. The long-term frontal *frequency maps* show the pixel-based frequency F of fronts normalized on cloudiness: For each pixel, F = N/C, where N is the number of times the given pixel contained a front, and C is the number of times the pixel was cloud-free. Thus, the frequency maps are best suited for displaying most stable fronts. At the same time, frontal frequency maps understate some fronts associated with widely meandering currents such as the Gulf Stream Extension, North Atlantic Current, and Azores Current. In such cases quasi-synoptic frontal *composite maps* are most helpful because they present all of the synoptic snapshots of the "instant" fronts detected in individual SST images within a given time period (e.g. week, month, or season), without any averaging or smoothing. The frontal composite maps thus allow one to detect the most unstable fronts that are not conspicuous in the frontal frequency maps. The *long-term frontal gradient maps* show two scalar quantities, *gradient magnitude* and *gradient direction*, associated with each frontal pixel in the long-term frontal frequency maps. Gradient visualization by color mapping gradient magnitude and direction (e.g. Ullman and Cornillon, 1999) has a clear advantage over vector mapping, namely resolution. Scalar mapping allows even tiny details to be preserved, down to a single pixel, whereas vector mapping typically requires subsampling, otherwise vector maps become crowded and illegible.

GULF OF ALASKA

Fronts in the **Gulf of Alaska** vary strongly with season and year. In late fall-winter, the **Shelf-Slope Front (SSF)** is observed in the northern and northwestern Gulf that peaks in February-April between 140°W and 165°W, extending from Queen Charlotte Islands in the east up to Shumagin Islands in the west (**Figure 1**). This front is associated with the Alaskan Stream (e.g. Reed and Schumacher, 1987)). In winter, the Alaskan Stream seems to be bounded by *two* parallel fronts. Such situations were clearly recorded in March 1987, April and December 1992, January and March 1995, and March 1996; less clearly, in February 1986 and March-April 1990. The SSF seems to sporadically form a **large meander off Kodiak Island at 148-150°W**, first described by Musgrave et al. (1992) who correctly (albeit tentatively) mapped it from a single hydrographic section in April 1988 augmented by

drifter observations. Our frontal composite maps for April and May 1988 revealed the same meander and confirmed the mapping by Musgrave et al. (1992). Moreover, we have identified similar meanders in February 1989, December 1992, and March 1993. From May through July, the Gulf is full of short frontal segments that do not form any pattern. This is the season when the new upper mixed layer is thin and the density difference across the new seasonal thermocline is small, hence the upper layer and seasonal thermocline could be easily mixed by a storm. Thus, any fronts that appear in the new upper mixed layer are bound to be short-lived.

In August-September, **a newly found 'horseshoe' front** east of Kodiak Island is prominent that persists through November (**Figure 2**). This front consists of two parts, (1) zonal front along ~59°N, east of Barren Islands and north of Portlock Bank, and (2) outer shelf-slope front along the shelf break/upper slope (SSF). The **zonal front** is apparently associated with the ACC which flows westward into Cook Inlet. Indeed, a CTD section in October 1991 along a quasi-meridional 151°W line has revealed a westward geostrophic jet at 59°N (Stabeno et al., 1995); our frontal SST map from the same month has shown a very stable zonal front at 59°N, collocated with the concurrent hydrography. The front bounds the relatively warm inshore waters diluted by the Kenai Peninsula runoff, hence the old term the 'Kenai Current' (Schumacher and Reed, 1980), later replaced by the 'Alaska Coastal Current' (Royer, 1981; Reed and Schumacher, 1987). The front is distinct from May through November and is best defined in late summer and fall. The front maintenance/intensification might be partially accounted for by the tides that are known to completely mix the water column over Portlock Bank, south of the front (Reed and Schumacher, 1987, Figure 3-10). The **outer shelf-slope front (SSF)** is apparently associated with the Alaskan Stream. This front is prominent from August through October when, together with the above zonal front, it dominates the Gulf's frontal pattern (**Figure 1**).

A **shelf front SW of Kodiak Island** was sporadically observed from February through May (in 1985, 1986, 1990, 1991, and 1996) when it extended from Trinity Islands (154°W) up to 158°W where it joined the ACC. Another **front in the lee of Kodiak Island, NE of Chirikof Island** was observed for one or two months in late summer, between July and October. Both features have not been described before. It is not clear at this point if there is any relation between these fronts. Both fronts might have some relevance to the southwestward outflow from the Shelikof Strait observed from drifters (Schumacher and Kendall, 1991) and reproduced in a model (Hermann and Stabeno, 1996; Stabeno and Hermann, 1996). Since these fronts are neither seasonally persistent nor spatially stable, they do not show up in long-term frontal frequency maps but are distinct in quasi-synoptic frontal composite maps for individual months. Both fronts might play an important role in the life cycle of walleye pollock because the adult migration to the spawning ground in the lower Shelikof Strait and the subsequent larvae drift out of Shelikof Strait (as shown by Schumacher and Kendall (1995, Figure 1)) take place in the immediate vicinity of these fronts.

Thomson and Gower (1998) reported a "train" of six eddies in March 1995 between Queen Charlotte Islands and Kayak Island. Our front detection algorithm correctly identified the offshore rims of these eddies as fronts connected to each other in a way reminiscent of Thomson and Gower (1998, Figure 1). Moreover, we found evidence of similar wave/eddy train patterns in February 1989, March-April 1990, April-May 1992, and March and May 1996. Thus, **the instability events that cause the observed eddy/wave trains might be quite typical of the wintertime regime of the Gulf of Alaska**.

Using nine clear AVHRR images from 1983, Thomson and Emery (1986) have observed a narrow along-shore poleward current off British Columbia, termed the **Haida Current**, between October and April. From cloud-free 1-km resolution AVHRR images between July 1987 and September 1991, Jardine et al. (1993) noticed the Haida Current in summer too, albeit rarely. Our declouding algorithm allowed even partly cloudy images to be used in front detection and tracking. As a result, the **Haida Front was distinguished from September through March**. Alternative explanations of the improved visibility of the front implicate a regime shift after 1983 or a strong interannual variability of the front, with the year of 1983 being a poor visibility year. Note that our front tracking algorithm consistently detected the Haida Front despite its relatively weak SST signal, up to 1°C in the Haida Current core (Thomson and Emery, 1986).

A **well-defined front was observed in Hekate Strait (~131°W) from July through March** (**Figure 2**). The front is best defined in September, when it extends along the eastern

coasts of the Queen Charlotte Islands between 52.5°-54°N. The front's northern part is the **Dogfish Banks Front** (east of the islands), interpreted by Jardine et al. (1993) as a tidal mixing front. They observed this front to reverse seasonally, with the on-bank water being 1-2°C colder in winter and 2-3°C warmer in summer than the off-bank water. The seasonal reversal is explained by the Banks' shallowness, with the front located over the 20-30-m depths (Jardine et al., 1993). This front has the maximum near-surface concentrations of Chl-a, nutrients, diatoms and copepods relative to ambient waters (Perry et al., 1983). Other local fronts reported by Jardine et al. (1993) and Crawford et al. (1995) have also been sporadically observed, including the mainland coastal upwelling front in eastern Hekate Strait, a semi-circular front associated with the Moresby Eddy in southern Hekate Strait/Queen Charlotte Sound and the Cape Scott upwelling front NW of Vancouver Island.

BERING SEA

The fronts' importance in the Bering Sea is well documented, especially in its ***southeastern part*** that features three prominent fronts, *inner*, *middle*, and *outer*, that correspond roughly to the 50, 100, and 170-m (shelf break) isobaths respectively (Kinder and Coachman, 1978; Schumacher et al., 1979; Coachman at al., 1980; Kinder and Schumacher, 1981a; Coachman, 1986; Schumacher and Stabeno, 1998). Tides are important, especially over the Bering Sea shelf (Kowalik, 1999), where strong *tidal mixing fronts* (TMF) are observed to completely surround main islands of the Pribilof Archipelago (Schumacher et al., 1979; Kinder et al., 1983; Brodeur et al., 1997, 2000). The fronts play a key role as principal biogeographical boundaries. They separate distinct biotopes (Iverson et al., 1979; Vidal and Smith, 1986) and at the same time they are biotopes *per se* (Kinder et al., 1983; Hansell et al., 1989; Russell et al., 1999). The primary and secondary biological productivity is enhanced at fronts that attract fish, birds, and mammals, including whales (Schneider, 1982; Schneider et al., 1987; Moore et al., 1995; Springer et al., 1996; Russell et al., 1999).

Our knowledge of these fronts is, however, rudimentary, except for, perhaps, the SE Bering Sea. Much less is known, however, about fronts of the ***northern Bering Sea*** (e.g. Gawarkiewicz et al., 1994). The northern Bering Sea fronts are intimately related to the SE Bering Sea fronts since the mean along-front flows are northwestward (Kinder and Schumacher, 1981b) so that northern fronts are essentially downstream extensions of the southern fronts (e.g. Coachman, 1986). In the same time, the northern Bering Sea frontal pattern continues to the Chukchi Sea via the Bering Strait. This connection is highly important: A large amount of nutrients and phytoplankton is brought by the Bering Slope Current associated with the shelf break front to the Gulf of Anadyr, from where it is transported by the Anadyr Current to the Chirikov Basin and eventually to the Chukchi Sea (Hansell et al., 1989; Walsh et al., 1997).

Notwithstanding the overwhelming importance of fronts in physical and biological processes that evolve in the Bering Sea, a reliable climatology of fronts is absent. The fronts' association with bottom topography and relations to principal ocean-atmosphere variables (ice, air temperature, wind, runoff, and Bering Strait exchange) has not been studied. The seasonal, interannual and decadal variability of the fronts are expected to correlate with the above-mentioned environmental parameters. For example, some of the fronts are located near the maximum extent of the sea ice cover, which fluctuates widely on the interannual time scale, between "warm" and "cold" years, with minimum and maximum development of the sea ice cover respectively (Niebauer, 1998; Wyllie-Echeverria and Ohtani, 1999). Consequently, parameters of such fronts are expected to be different during "warm" and "cold" years. Possible "*regime shifts*" in the study area's frontal pattern and its characteristics might be linked to the known regime shifts in the North Pacific (Graham, 1994; Polovina et al., 1994; Niebauer, 1998; Brodeur et al., 1999).

The Bering Sea frontal pattern changes dramatically as the season progresses. The frontal pattern in May (**Figure 3**) features a well-defined ridge of elevated frontal frequencies extended from Bristol Bay westward to Cape Navarin. The ridge is not isobathic, so the corresponding front is located over shallow depths (~50 m) in Bristol Bay but continues over the outer shelf (100-200 m depth) in the northwestern part of the sea. Hence the front location does not correspond to any of the major known fronts (inner, middle, or outer) since these fronts are believed to be isobathic (e.g. Coachman, 1986). The front configuration is however remarkably similar to the sea ice cover's edge in May; the edge is located about 1° of latitude to the north of the front (Gloersen et al., 1992; NASA, 1998). The front thus appears to be related to the marginal ice zone processes (Muench and Schumacher, 1985) and represents

an imprint left in the ocean by the receding sea ice cover.

In November, the frontal pattern is different (**Figure 4**). Instead of one major front, several fronts extend essentially in the same SE-NW direction over the shelf break, outer shelf and inner shelf. Some inner shelf fronts are observed well inshore of the 50-m isobath, so they are not necessarily related to the tidal mixed front believed to be associated with the 50-m isobath (e.g. Coachman, 1986). Two fronts are distinct in the northwest that correspond to the northward Anadyr Current and southward Kamchatka Current, branches of the Bering Slope Current.

CHUKCHI SEA

Long-term (1985-1996) August and September frontal probability maps (**Figures 5 and 6**) show a number of features in the Chukchi Sea at the peak of summer. Some of the features are easily identifiable, whereas others might represent newly found fronts (a caveat: based on satellite data alone, the below interpretations are tentative). Front 1 corresponds to the Bering Strait inflow that makes a quasi-stationary incursion into Kotzebue Sound. Farther north, front 2 extends zonally toward Point Barrow. This front might be an eastward extension of front 3 or 4 (**Figure 7**). Front 3 is the most robust; the front's stability is accounted for by the strict topographic control: The front hugs the steep southern flank of Herald Shoal. Front 4 is associated with the Chukotkan segment of the Siberian Coastal Current, SCC, mapped by Weingartner et al. (1999) whose in situ dataset included CTD sections occupied during the same month (September 1995) as the satellite data used in **Figure 7**. Front 5 is best defined in September (**Figures 6 and 7**) when it emerges as a northeastward extension of the SCC that veers offshore around Wrangel Island to pass through Herald Valley, then continues eastward at ~72°N north of Herald Shoal, as shown by Weingartner et al. (1999). An intriguing discrepancy between our results and Weingartner et al. (1999) is that front 5 in **Figure 7** veers offshore immediately downstream of Long Strait, not in the southern Chukchi Sea as shown in the SCC schematic by Weingartner et al. (1999, Fig.1). The reason for this discordance is unclear. Past Herald Valley, front 5 is roughly parallel to sea ice edge, being located ~100 km south of the latter, according to the NASA September 1995 sea ice data available from NSIDC.

BEAUFORT SEA

Frontal structure and processes in this region remain largely unexplored since the pioneering study by Carmack et al. (1989). These fronts can be divided in three basic types: (1) riverine (estuarine), e.g. the Mackenzie River Plume fronts; (2) shelf break front, (3) marginal ice zone fronts. The Mackenzie River empties into the Beaufort Sea through three channels, hence three plumes are expected, interacting with each other and with other fronts. The Mackenzie River runoff and sediment discharge are, respectively, the fourth and the largest in the Arctic Ocean. Under favorable ice/wind conditions, the Mackenzie River plume can spread across the Canadian shelf and extend well into the open ocean, as far as 400 km away from its source, being clearly visible in satellite imagery (Macdonald et al., 1999). Therefore plume front studies should help elucidate mechanisms of pollutant, sediment, and tracer dispersal across the Arctic Ocean shelves and beyond. The shelf break front (SBF) of the Beaufort Sea is evident in satellite SST data (**Figures 8 and 9**). It is noteworthy that the SBF attains its maximum robustness off Bathurst Peninsula where the continental slope is the steepest. Clearly, the topography steers the SBF. The Bathurst Polynya coincides with the location of the maximum frequency of the SBF. This is the location where many marine mammals congregate such as walruses, belugas etc.

The Mackenzie Canyon area has never been a subject of a three-dimensional oceanographic survey although several hydrographic sections were occupied in its vicinity (e.g. O'Rourke, 1974; Carmack et al., 1989). A year-long mooring installed in the canyon revealed 400-m vertical isopycnal displacements caused by wind-induced upwelling (Carmack and Kulikov, 1998). The ambient large-scale circulation appears highly dynamics and is poorly known (Carmack and Macdonald, 2001). The area is located on the southern periphery of the Beaufort Sea where the canonical anticyclonic circulation of the Beaufort Gyre is replaced by a weak cyclonic circulation (Wilson, 1974). The surface layer circulation is mostly wind-driven although the Mackenzie River Plume creates density contrasts that cause geostrophic flows. The plume distribution is, however, governed by wind (in the absence of wind, the plume turns northeast due to Coriolis force), therefore wind appears to dominate the surface circulation. The Mackenzie River does not form a single, coherent plume. On the contrary, several distinct temperature, salinity, and turbidity

fronts are present on the Mackenzie Shelf at any given time (Carmack et al., 1989). These fronts are important feeding and nursery grounds for fish, sea birds, seals and cetaceans. In those rare occasions when observations on marine mammals were augmented by physical oceanography measurements marine mammals were found to congregate at oceanic fronts (Borstad, 1985; Bradstreet et al., 1987; Moore et al., 1995). Under favorable ice/wind conditions, the Mackenzie plume spreads across the Canadian shelf and extends well into the open ocean, sometimes as far as 400 km away from its source, being clearly visible in satellite imagery (Macdonald et al., 1999).

ACKNOWLEDGMENTS

This research was supported by the NASA grants No. 535834 and No. 535835 and the NOAA grant No. 537430. The support of both agencies is greatly appreciated.

REFERENCES

Ahlnäs, K., and G.R. Garrison (1984) Satellite and oceanographic observations of the warm coastal current in the Chukchi Sea, *Arctic*, *37*(3), 244-254.

Belkin, I.M., R. Krishfield and S. Honjo (2002) Decadal variability of the North Pacific Polar Front: Subsurface warming versus surface cooling, *Geophys. Res. Lett.*, **29**(9), doi: 10.1029/2001GL013806.

Belkin, I.M. (2003a) Front, in: *The Encyclopedia of Oceanography*, Taylor and Francis, New York, in press.

Belkin, I.M. (2003b) Ocean Fronts, in: *The Encyclopedia of the Arctic*, edited by Mark Nuttall, Taylor and Francis, New York, in press.

Belkin, I.M., P. Cornillon, D. Ullman, and Z. Shan (2003a) Global pattern of ocean fronts from Pathfinder SST data: I. Atlantic Ocean, in preparation.

Belkin, I.M., P. Cornillon, D. Ullman, and Z. Shan (2003b) Global pattern of ocean fronts from Pathfinder SST data: II. Pacific Ocean, in preparation.

Belkin, I.M., P. Cornillon, D. Ullman, and Z. Shan (2003c) Global pattern of ocean fronts from Pathfinder SST data: III. Indian Ocean, in preparation.

Borstad, G.A. (1985) Water colour and temperature in the southern Beaufort Sea: Remote sensing in support of ecological studies of the bowhead whales, Can. Tech. Rep. Fish. Aquat. Sci., No. 1350, 73 pp.

Bradstreet, M.S.W., D.H. Thompson, and D.B. Fissel (1987) Zooplankton and bowhead whale feeding in the Canadian Beaufort Sea, 1986, *Environ. Stud. (Can., Dept. Indian Aff. North. Dev.)*, **50**, 1-204.

Brodeur, R.D., M.T. Wilson, and J.M. Napp (1997) Distribution of juvenile pollock relative to frontal structure near the Pribilof Islands, Bering Sea, in: *Forage Fishes in Marine Ecosystems*, pp. 573-589, Proc. Int'l Symp. on the Role of Forage Fishes in Marine Ecosystems, Alaska Sea Grant College Program Rep. No. 97-01, University of Alaska Fairbanks.

Brodeur, R.D., C.E. Mills, J.E. Overland, G.E. Walters, and J.D. Schumacher (1999) Evidence for a substantial increase in gelatinous zooplankton in the Bering Sea, with possible link to climate change, *Fish. Oceanogr.*, *8*(4), 296-306.

Brodeur, R.D., M.T. Wilson, and L. Ciannelli (2000) Spatial and temporal variability in feeding and condition of age-0 walleye pollock (*Theragra chalcogramma*) in frontal regions of the Bering Sea, *ICES J. Mar. Sci.*, *57*(2), 256-264.

Carmack, E.C., and Y.A. Kulikov (1998) Wind-forced upwelling and internal Kelvin wave generation in Mackenzie Canyon, Beaufort Sea, *J. Geophys. Res.*, **103**(C9), 18447-18458.

Carmack, E.C., R.W. Macdonald, and J.E. Papadakis (1989) Water mass structure and boundaries in the Mackenzie Shelf estuary, *J. Geophys. Res*., **94**(12), 18043-18055.

Carmack, E.C., and R.W. Macdonald (2002) Oceanography of the Canadian Shelf of the Beaufort Sea: A setting for marine life, *Arctic*.

Cayula, J.-F., Cornillon, P. (1992) Edge detection algorithm for SST images. *J. Atmos. Oceanic Tech.*, *9*(1), 67-80.

Cayula, J.-F., Cornillon, P. (1995) Multi-image edge detection for SST images. *J. Atmos. Oceanic Tech.*, *12*(4), 821-829.

Cayula, J.-F., Cornillon, P. (1996) Cloud detection from a sequence of SST images. *Remote Sensing of Environment*, *55*(1), 80-88.

Coachman, L.K., T.H. Kinder, J.D. Schumacher, and R.B. Tripp (1980) Frontal systems of the southeastern Bering Sea shelf, in: *Second International Symposium on Stratified Flows*,

vol. 2, edited by T. Carstens and T. McClimans, pp. 917-933, Tapir, Trondheim.

Coachman, L.K. (1986) Circulation, water masses, and fluxes on the southeastern Bering Sea shelf, *Cont. Shelf Res.*, *5*(1/2), 23-108.

Crawford, W.R., M.J. Woodward, M.G.G. Foreman, and R.E. Thomson (1995) Oceanographic features of Hecate Strait and Queen Charlotte Sound in summer, *Atmosphere-Ocean*, *33*(4), 639-681.

Favorite, F., Dodimead, A.J., and Nasu, K. (1976) Oceanography of the Subarctic Pacific region. *Bulletin of the International North Pacific Fisheries Commission*, *33*, 187 pp.

Fedorov, K.N. (1986) The Physical Nature and Structure of Oceanic Fronts. Springer-Verlag, Berlin etc., viii+333 pp.

Gawarkiewicz, G., J.C. Haney, and M.J. Caruso (1994) Summertime synoptic variability of frontal systems in the northern Bering Sea, *J. Geophys. Res.*, *99*(C4), 7617-7625.

Gloersen, P., Campbell, W.J., Cavalieri, D.J., Comiso, J.C., Parkinson, C.L., and Zwally, H.J. (1992) Arctic and Antarctic Sea Ice, 1978-1987: Satellite Passive-Microwave Observations and Analysis. NASA SP-511, Washington, D.C., 290 pp.

Graham, N.E. (1994) Decadal-scale climate variability in the Tropical and North Pacific during the 1970s and 1980s: Observations and model results. *Climate Dynamics*, *10*(3), 135-162.

Hansell, D.A., J.J. Goering, J.J. Walsh, C.P. McRoy, L.K. Coachman, and T.E. Whitledge (1989) Summer phytoplankton production and transport along the shelf break in the Bering Sea, *Cont. Shelf Res.*, *9*(12), 1085-1104.

Hermann, A.J., and P.J. Stabeno (1996) An eddy resolving model of circulation on the western Gulf of Alaska shelf: 1. Model development and sensivity analyses, *J. Geophys. Res., 101*(C1), 1129-1149.

Hickox, R., I.M. Belkin, P. Cornillon, and Z. Shan (2000) Climatology and seasonal variability of ocean fronts in the East China, Yellow and Bohai Seas from satellite SST data, *Geophys. Res. Lett.*, *27*(18), 2495-2498.

Iverson, R.L., L.K. Coachman, R.T. Cooney, T.S. English, J.J. Goering, G.L. Hunt, Jr., M.C. Macauley, C.P. McRoy, W.S. Reeburg, T.E. Whitledge, and R.J. Livingston (1979) Ecological significance of fronts in the southeastern Bering Sea, in: *Ecological Processes in Coastal and Marine Systems*, pp. 437-468, Plenum Press, London.

Jardine, I.D., K.A. Thomson, M.G. Foreman, and P.H. LeBlond, Remote sensing of coastal sea-surface features off northern British Columbia, *Remote Sens. Environ.*, *45*(1), 73-84.

Kazmin, A.S., and Rienecker, M.M. (1996) Variability and frontogenesis in the large-scale oceanic frontal zones. *J. Geophys. Res.*, *101*(C1), 907-921.

Kinder, T.H., and L.K. Coachman (1978) The front overlaying the continental slope in the eastern Bering Sea, *J. Geophys. Res.*, *83*(C9), 4551-4559.

Kinder, T.H., and J.D. Schumacher (1981a) Hydrographic structure over the continental shelf of the southeastern Bering Sea, in: *The Eastern Bering Sea Shelf: Oceanography and Resources*, Volume 1, edited by D.W. Hood and J.A. Calder, pp. 31-52, NOAA, University of Washington Press, Seattle.

Kinder, T.H., and J.D. Schumacher (1981b) Circulation over the continental shelf of the southeastern Bering Sea, in: *The Eastern Bering Sea Shelf: Oceanography and Resources*, Volume 1, edited by D.W. Hood and J.A. Calder, pp. 53-75, NOAA, University of Washington Press, Seattle.

Kinder, T.H., G.L. Hunt, Jr., D. Schneider, D., and J.D. Schumacher (1983) Correlations between seabirds and oceanic fronts around the Pribilof Islands, Alaska, *Estuarine, Coastal and Shelf Science*, *16*(3), 303-319.

Kowalik, Z. (1999) Bering Sea tides, in: *Dynamics of the Bering Sea*, edited by T.R. Loughlin and K. Ohtani, pp. 93-127, University of Alaska Sea Grant, AK-SG-99-03, Fairbanks.

Legeckis, R. (1978) A survey of worldwide sea surface temperature fronts detected by environmental satellites. *J. Geophys. Res.*, *83*(C9), 4501-4522.

Lynch, A.H., M.F. Glueck, W.L. Chapman, D.A. Bailey, and J.E. Walsh (1997) Satellite observation and climate system model simulation of the St. Lawrence Island polynya, *Tellus*, *49A*(2), 277-297.

Macdonald, R.W., E.C. Carmack, F.A. McLaughlin, K.K. Falkner, and J.H. Swift (1999) Connections among ice, runoff and atmospheric forcing in the Beaufort Gyre, *Geophysical Research Letters*, **26**(15), 2223-2226.

Maynard, N.G., and D.K. Clark (1987) Satellite color observations of spring blooming in Bering Sea shelf waters during the ice edge retreat in 1980, *J. Geophys. Res.*, *92*(C7), 7127-7139.

Moore, S.E., J.C. George, K.O. Coyle, and T.J. Weingartner (1995) Bowhead whales along the Chukotka coast in autumn, *Arctic*, **48**(2), 155-160.

Muench, R.D., and J.D. Schumacher (1985) On the Bering Sea ice edge front, *J. Geophys. Res.*, *90*(C2), 3185-3197.

Musgrave, D.L., T.J. Weingartner, and T.C. Royer (1992) Circulation and hydrography in the northwestern Gulf of Alaska, *Deep-Sea Res.*, *39*(9), 1499-1519.

NASA (1998) Sea ice concentrations from Nimbus-7 SMMR and DMSP SSM/I passive microwave data, 1978-1996, Volumes 1-3 (on CD-ROMs; USA_NASA_971_0001, 0002, 0003), Goddard Space Flight Center, Laboratory for Hydrospheric Processes. Archived and distributed by NSIDC, CIRES, University of Colorado Boulder.

Niebauer, H.J. (1998) Variability in Bering Sea ice cover as affected by a regime shift in the North Pacific in the period 1947-1996, *J. Geophys. Res.*, *103*(C12), 27717-27737.

O'Rourke, J.C. (1974) Inventory of physical oceanography of the eastern Beaufort Sea, in: *The Coast and Shelf of the Beaufort Sea*, pp. 65-84, edited by J.C. Reed and J.E. Sater, AINA, Arlington, VA.

Perry, R.I., B.R. Dilke, and T.R. Parsons (1983) Tidal mixing and summer plankton distributions in Hecate Strait, British Columbia, *Can. J. Fish. Aquat. Sci.*, *40*(7), 871-887.

Ray, R. (2000) M2 tidal energy dissipation, http://earthobservatory.nasa.gov/Newsroom /NewImages /Images /dissipation_large.jpg

Reed, R.K., and J.D. Schumacher (1987) Physical oceanography, in: The Gulf of Alaska, physical environment and biological resources, edited by D.W. Hood and S.T. Zimmerman, pp. 57-75, U.S. Department of Commerce and U.S. Department of the Interior, U.S. Gov. Printing Office, NTIS #PB87-103230.

Royer, T.C. (1981) Baroclinic transport in the Gulf of Alaska, II. Freshwater-driven coastal current, *J. Mar. Res.*, *39*(2), 251-266.

Russell, R.W., N.M. Harrison, N.M., and G.L. Hunt, Jr. (1999) Foraging at a front: Hydrography, zooplankton, and avian planktivory in the northern Bering Sea, *Mar. Ecol. Prog. Ser.*, *182*, 77-93.

Saitoh, S.-I., D. Eslinger, H. Sasaki, N. Shiga, T. Odate, and T. Miyoi (1998) Satellite and ship observations of coastal upwelling in the St. Lawrence Island Polynya (SLIP) area in summer, 1994 and 1995, *Mem. Fac. Fish. Hokkaido Univ.*, *45*(1), 18-23.

Schneider, D. (1982) Fronts and seabird aggregations in the southeast Bering Sea, *Mar. Ecol. Prog. Ser.*, *10*(1), 101-103.

Schneider, D., N.M. Harrison, and G.L. Hunt, Jr. (1987) Variation in the occurrence of marine birds at fronts in the Bering Sea, *Estuarine, Coastal and Shelf Science*, *25*(1), 135-141.

Schumacher, J.D., T.H. Kinder, D.J. Pashinski, and R.L. Charnell (1979) A structural front over the continental shelf of the eastern Bering Sea, *J. Phys. Oceanogr.*, *9*(1), 79-87.

Schumacher, J.D., and R.K. Reed (1980) Coastal flow in the northwest Gulf of Alaska: the Kenai Current, *J. Geophys. Res.*, *85*(C11), 6680-6688.

Schumacher, J.D., and A.W. Kendall, Jr. (1991) Some interactions between young walleye pollock and their environment in the western Gulf of Alaska, *CalCOFI Rep.*, *32*, 22-40.

Schumacher, J.D., and A.W. Kendall, Jr. (1995) An example of fisheries oceanography: Walleye pollock in Alaskan waters, *Rev. Geophys.*, *33*(suppl.), 1153-1163.

Schumacher, J.D., and P.J. Stabeno (1998) Continental shelf of the Bering Sea, in: *The Sea*, vol. 11, edited by A.R. Robinson and K.H. Brink, pp. 789-822, John Wiley and Sons, New York.

Springer, A.M., C.P. McRoy, and M.V. Flint (1996) The Bering Sea Green Belt: shelf-edge processes and ecosystem production, *Fish. Oceanogr.*, *5*(3/4), 205-223.

Stabeno, P.J., R.K. Reed, and J.D. Schumacher (1995) The Alaska Coastal Current: Continuity of transport and forcing, *J. Geophys. Res., 100*(C2), 2477-2485.

Stabeno, P.J., and A.J. Hermann (1996) An eddy resolving model of circulation on the western Gulf of Alaska shelf: 2. Comparison of results to oceanographic observations, *J. Geophys. Res., 101*(C1), 1151-1161.

Thomson, R.E. and W.J. Emery (1986) The Haida Current, *J. Geophys. Res.*, *91*(C1), 845-861.

Thomson, R.E., and J.F.R. Gower (1998) A basin-scale oceanic instability event in the Gulf of Alaska, *J. Geophys. Res., 103*(C2), 3033-3040.

Ullman, D.S. and P.C. Cornillon (1999) Surface temperature fronts off the East Coast of North America from AVHRR imagery, *J. Geophys. Res.*, *104*(C10), 23459-23478.

Ullman, D.S. and P.C. Cornillon (2000) Evaluation of front detection methods for satellite-derived SST data using in situ observations, *J. Atmos. Oceanic Tech.*, **17**(12), 1667-1675.

Ullman, D.S. and P.C. Cornillon (2001) Continental shelf surface thermal fronts in winter off the northeast U.S. coast, *Cont. Shelf Res.*, **21**(11-12), 1139-1156.

UNESCO (1992) Oceanic interdecadal climate variability, *IOC Technical Series*, *40*, 37 pp.

Vazquez, J., K. Perry, and K. Kilpatrick (1998) NOAA/NASA AVHRR Oceans Pathfinder sea surface temperature data set user's reference manual, Version 4.0. JPL Technical Report, D-14070; http://podaac.jpl.nasa.gov/pub/sea_surface_temperature/avhrr/pathfinder/doc/usr_gde4_0.html.

Vidal, J., and S.L. Smith (1986) Biomass, growth and development of populations of herbivorous zooplankton in the southeastern Bering Sea during spring, *Deep-Sea Res.*, *33*(4), 523-556.

Walsh, J.E., D.A. Dieterle, F.E. Muller-Karger, K. Aagaard, A.T. Roach, T.E. Whitledge, and D. Stockwell (1997) CO_2 cycling in the coastal ocean. II. Seasonal organic loading of the Arctic Ocean from source waters in the Bering Sea, *Cont. Shelf. Res.*, *17*(1), 1-36.

Weingartner, T.J., S. Danielson, Y. Sasaki, V. Pavlov, and M. Kulakov (1999) The Siberian Coastal Current: A wind- and buoyancy-forced Arctic coastal current, *J. Geophys. Res.*, **104**(C12), 29697-29713.

Wilson, H.P. (1974) Winds and currents in the Beaufort Sea, in: *The Coast and Shelf of the Beaufort Sea*, pp. 13-23, edited by J.C. Reed and J.E. Sater, AINA, Arlington, VA.

Wyllie-Echeverria, T., and K. Ohtani (1999) Seasonal sea ice variability and the Bering Sea ecosystem, in: *Dynamics of the Bering Sea*, edited by T.R. Loughlin and K. Ohtani, pp. 435-451, University of Alaska Sea Grant, AK-SG-99-03, Fairbanks.

Yuan, X., and Talley, L.D. (1996) The subarctic frontal zone in the North Pacific: Characteristics of frontal structure from climatological data and synoptic surveys. *J. Geophys. Res.*, *101*(C7), 16491-16508.

Figures

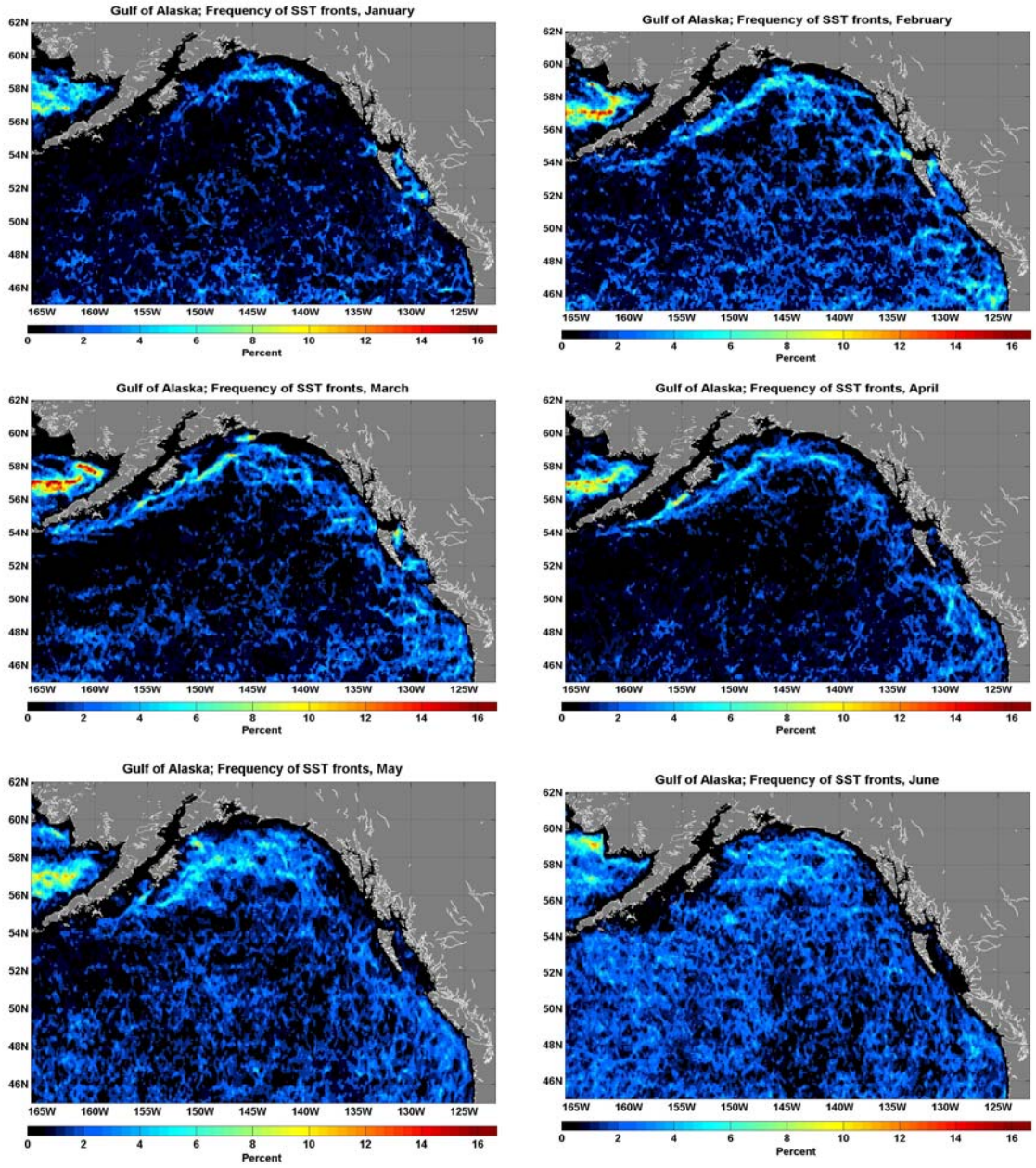

Figure 1. Long-term monthly frequency of SST fronts in the Gulf of Alaska, 1985-1996, January through June.

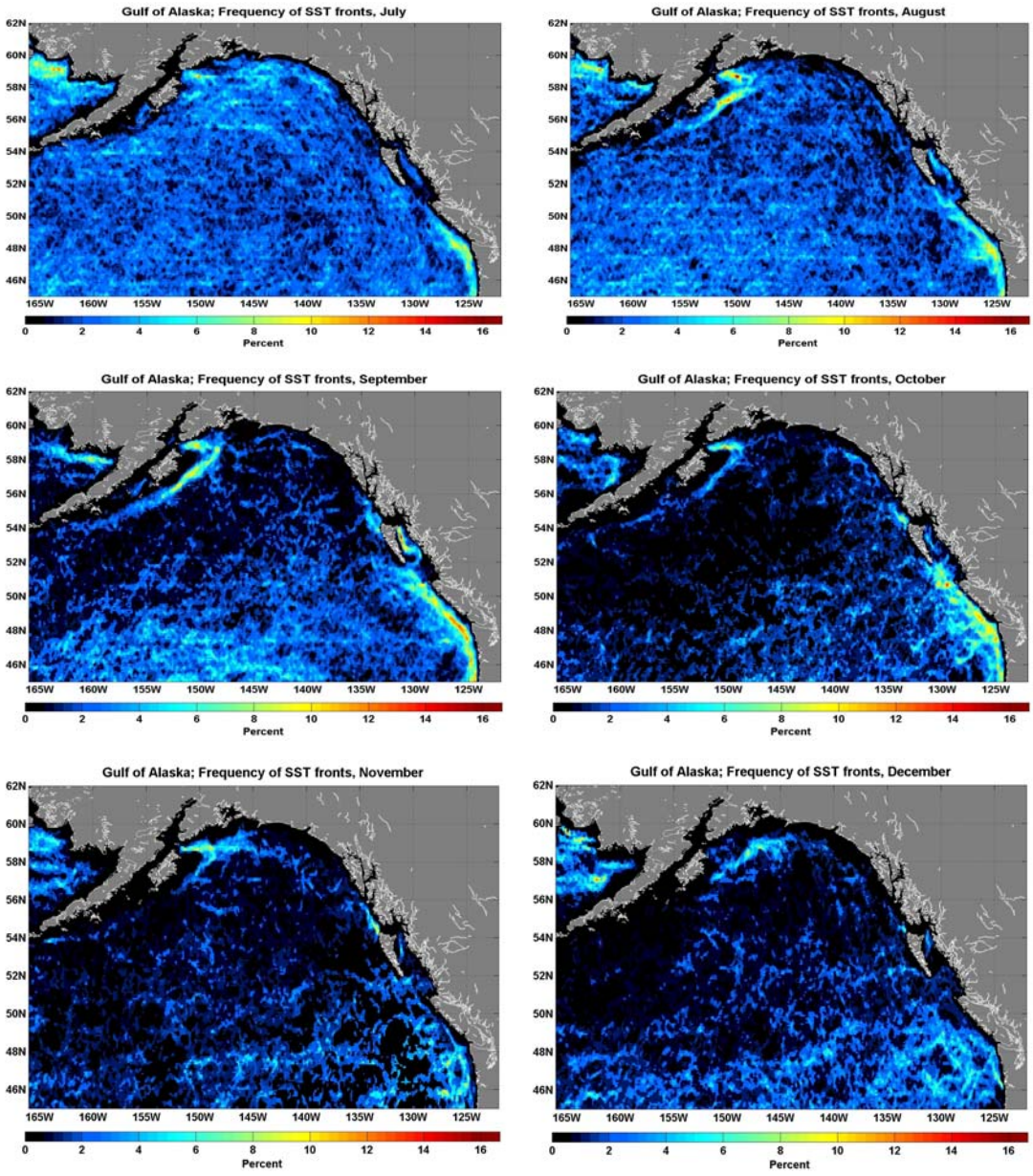

Figure 2. Long-term monthly frequency of SST fronts in the Gulf of Alaska, 1985-1996, July through December.

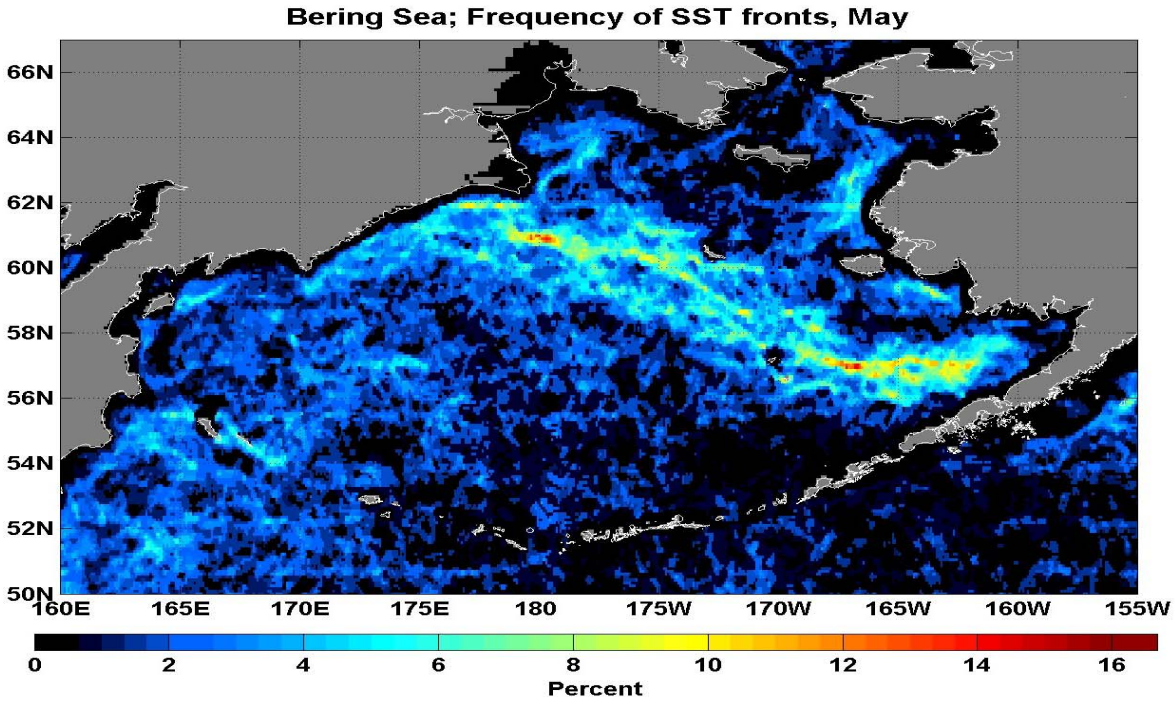

Figure 3. Long-term (1985-1996) May frequency of SST fronts in the Bering Sea.

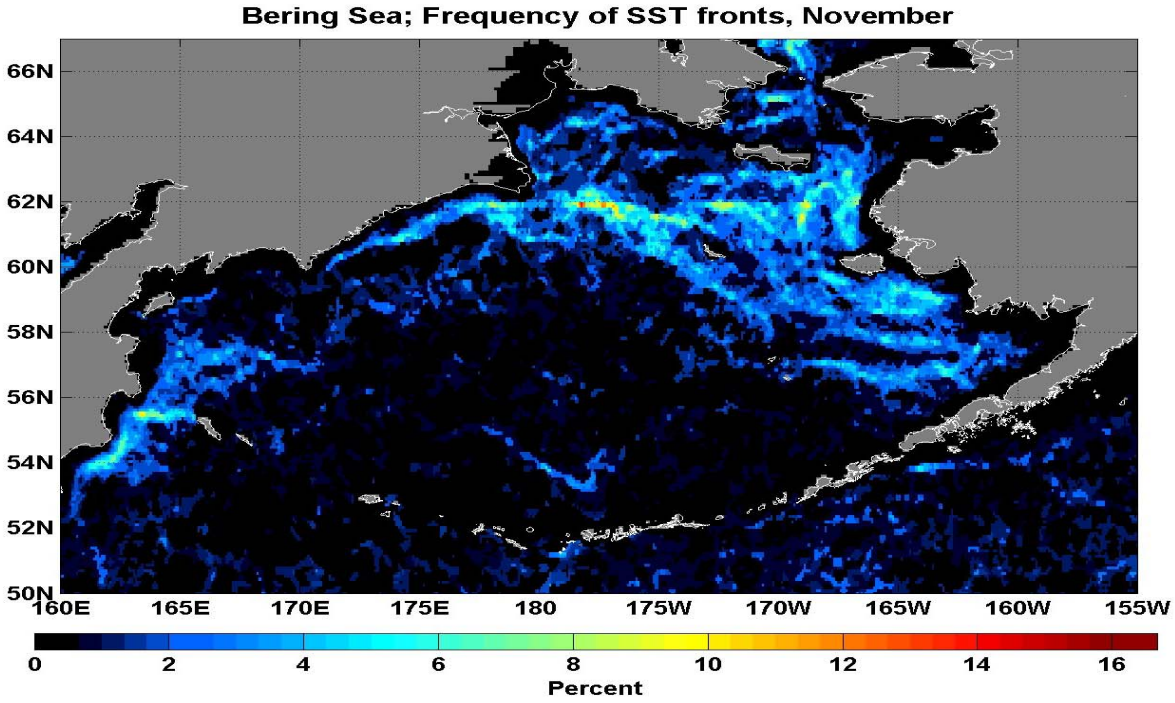

Figure 4. Long-term (1985-1996) November frequency of SST fronts in the Bering Sea.

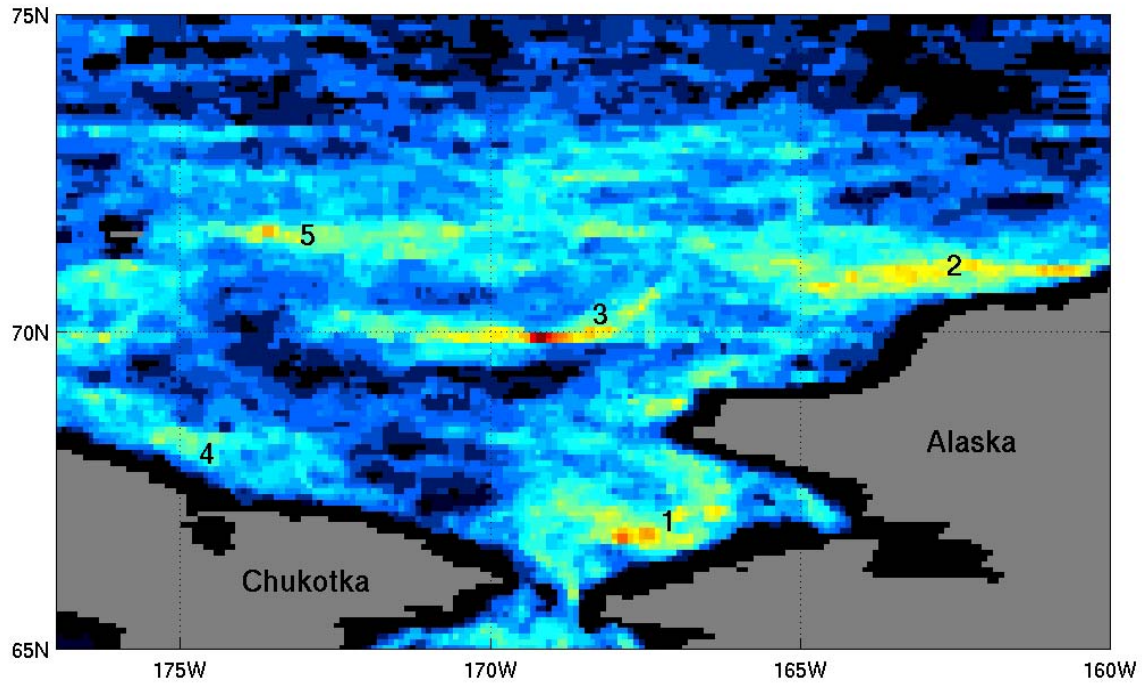

Figure 5. Long-term (1985-1996) August frequency of SST fronts, Chukchi Sea.

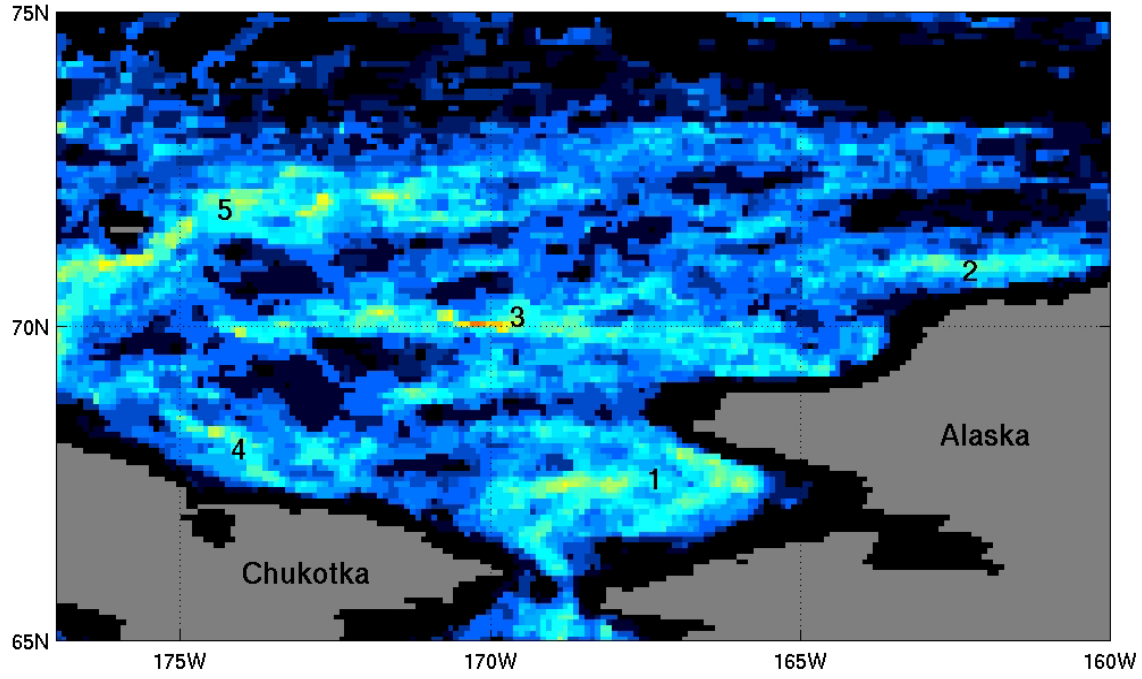

Figure 6. Long-term (1985-1996) September frequency of SST fronts, Chukchi Sea.

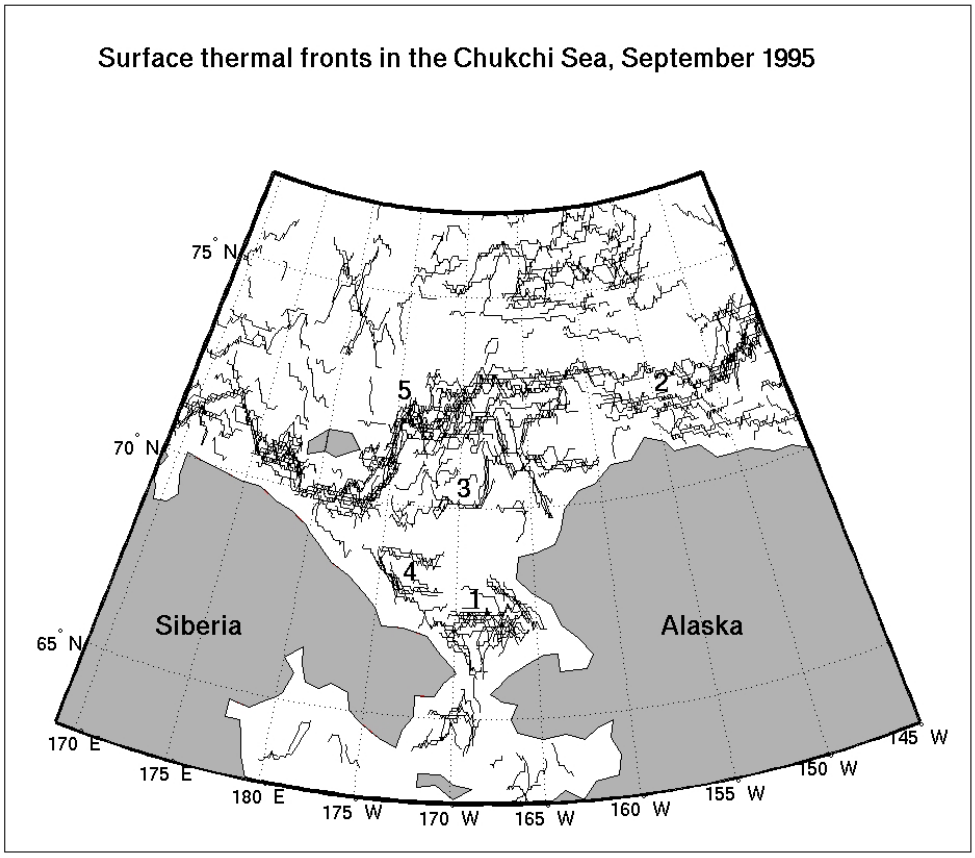

Figure 7. Quasi-synoptic composite map of SST fronts in the Chukchi Sea, September 1995. Front numbers correspond to Figures 5 and 6.

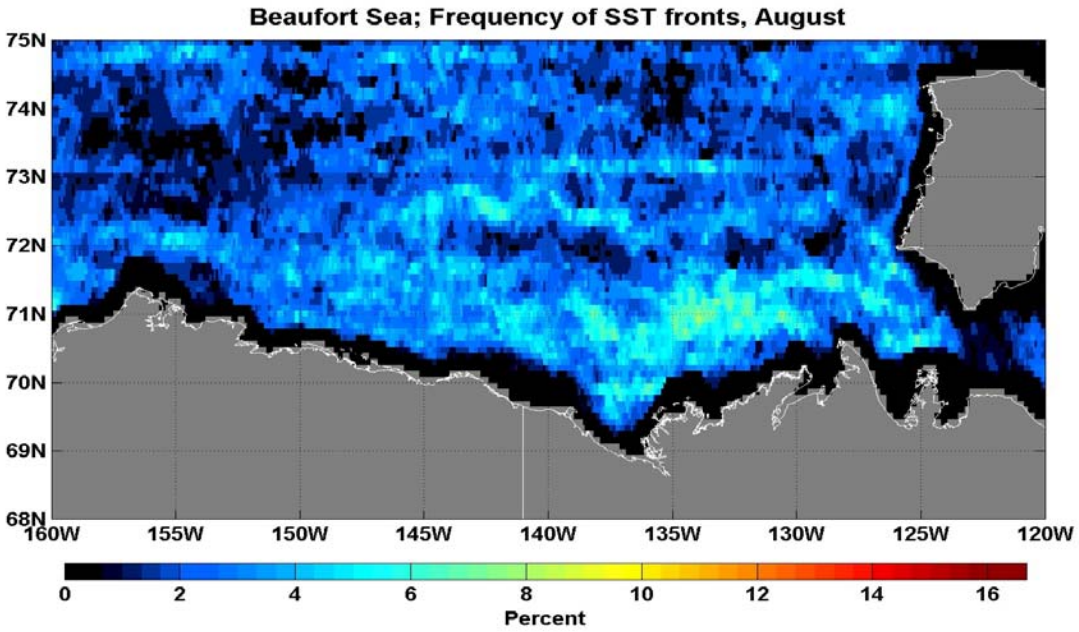

Figure 8. Long-term (1985-1996) August frequency of SST fronts in the Beaufort Sea. The shelf break front is evident at 130-135W.

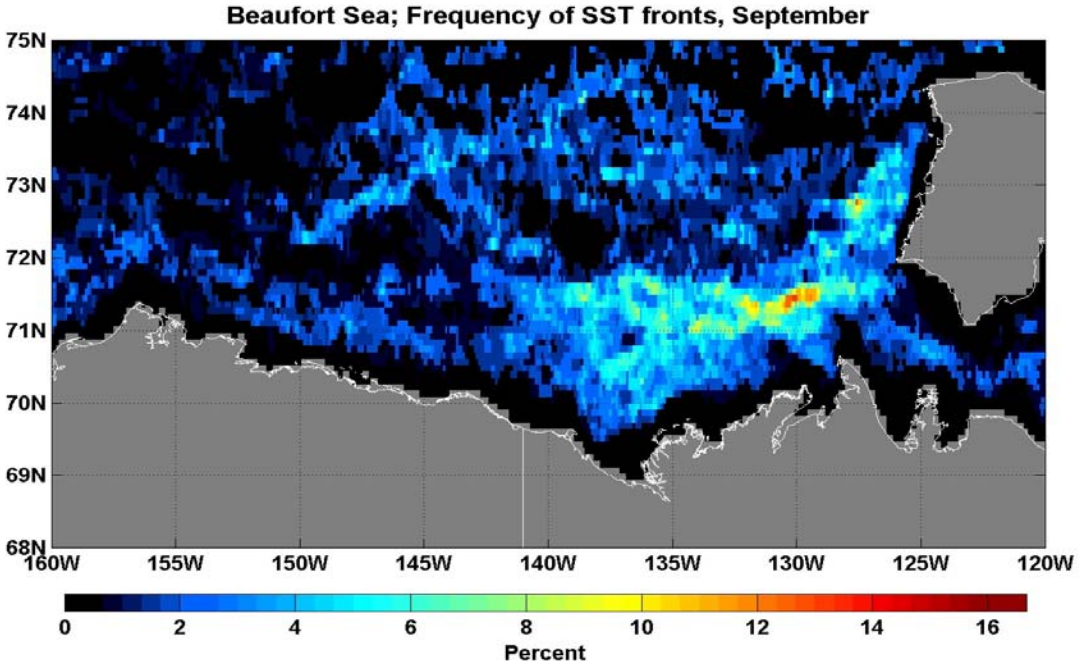

Figure 9. Long-term (1985-1996) September frequency of SST fronts in the Beaufort Sea. The shelf break front is evident at 130-135W.